Condensation in a steady-flow thermoacoustic refrigerator

R. A. Hiller[a] and G. W. Swift
Condensed Matter and Thermal Physics Group, Los Alamos National Laboratory, Los Alamos, New Mexico 87545

(Received 29 May 1999; accepted for publication 22 June 2000)

Condensation may occur in an open-flow thermoacoustic cooler with stack temperatures below the saturation temperature of the flowing gas. In the experimental device described here the flowing gas, which is also the acoustic medium, is humid air, so the device acts as a flow-through dehumidifier. The humid air stream flows through an acoustic resonator. Sound energy generated by electrodynamic drivers produces a high-amplitude standing wave inside of the resonator, which causes cooling on a thermoacoustic stack. Condensation of water occurs as the humid air passes through the stack and is cooled below its dew point, with the condensate appearing on the walls of the stack. The dry, cool air passes out of the resonator, while the condensate is wicked away from the end of the stack. Thermoacoustic heat pumping is strongly affected by the form of the condensate inside of the stack, whether condensed mostly on the stack plates, or largely in the form of droplets in the gas stream. Two simple models of the effect of the condensate are matched to a measured stack temperature profile; the results suggest that the thermoacoustic effect of droplets inside the stack is small. © *2000 Acoustical Society of America.* [S0001-4966(00)02210-4]

PACS numbers: 43.25.Ud [HEB]

I. INTRODUCTION

Superimposing steady flow with oscillating, or acoustic, flow in thermoacoustic engines and refrigerators promises to simplify the construction of these machines, and can lead to higher efficiency than conventional thermoacoustic designs.[1] In this arrangement the working fluid of the acoustic system is also the process fluid, which enters and exits the acoustic resonator at pressure nodes. If the working fluid is humid air and the stack temperature reaches the incoming dew point, condensation will occur in the stack. The condensed water flows along the stack plates, and may be collected and removed from the resonator. The flowing air stream exits the stack, and then the resonator, with a dew point equal to the temperature of the cold end of the stack. The result is dehumidification of the stream.[2]

Such a dehumidifier may have application in compressed-air drying, and in the drying of agricultural and industrial products. For example, it is possible to drive a thermoacoustic dehumidifier with a thermoacoustic prime mover to allow dehumidification powered by a flame or other heat source in remote locations.

To explore some of the issues involved in flow-through thermoacoustic dehumidification we have made measurements with humid air flowing through a loudspeaker-driven thermoacoustic cooler. The air stream is indeed dehumidified, simply and reliably, by this thermoacoustic apparatus. However, thus far the efficiency is much lower than that of commercial dehumidifiers based on vapor-compression refrigeration.

The steady flow velocity is small compared to acoustic velocities. The typical flow rate used is about 0.002 kg/s (each stack) at a static pressure of 300 kPa, which corresponds to a volume flow rate of about 10^{-3} m^3/s, or a velocity in a 15-cm-diam duct of 0.06 m/s, far smaller than the peak acoustic velocity of about 7 m/s. The steady flow may be viewed as a small drift of the fluid on top of the much larger acoustic oscillations. The steady flow does not directly affect the acoustics or thermoacoustics, but imposes an additional enthalpy flow.

For order-of-magnitude calculations a simple model of thermoacoustic heat pumping can be used to understand the heat flows and temperature gradient in a dehumidifying stack.[3] While quantitatively inaccurate, this model allows qualitative understanding of the effect of thermodynamic derivatives on the heat flows in the system, and (later in this article) why different models of the details of the condensation should make a large change in the estimated thermoacoustic heat pumping rates.

Reckoning distance z from the cold end of the stack towards the warm end, the boundary-layer approximation for thermoacoustic heat pumping in the stack is[3]

$$\dot{Q}_2 = \frac{1}{4}\Pi \delta_k T_m \beta p_1^s u_1^s \left(1 - \frac{dT_m/dz}{\nabla T_{\text{crit}}}\right) \tag{1}$$

if viscosity is neglected and the stack length is assumed to be so short that all relevant variables are essentially independent of z. Here Π is the total perimeter of the stack plates,

$$\delta_k = \sqrt{2K/\omega\rho_m c_p} \tag{2}$$

is the thermal penetration depth (the spacing between stack plates being typically a few δ_k), T_m is the mean, that is, time-averaged, temperature of the stack and fluid, β is the fluid's thermal expansivity, p_1^s and u_1^s are the (standing wave) acoustic pressure and velocity amplitudes, K is the fluid's thermal conductivity, ω is the acoustic radian frequency, ρ_m is the mean fluid density, and c_p is the heat

[a]Present address: Department of Physics and Astronomy, and National Center for Physical Acoustics, University of Mississippi, University, MS 38677.

capacity per unit mass at constant pressure. The critical temperature gradient is

$$\nabla T_{\text{crit}} = \omega T_m \beta p_1^s / \rho_m c_p u_1^s . \tag{3}$$

For this apparatus $\nabla T_{\text{crit}} \approx 150$ K/m, and $\dot{Q}_2$ at $dT_m/dz = 0$ is about 50 W.

With no steady flow the enthalpy flux down the stack is assumed to be equal to the thermoacoustic heat pumping $\dot{Q}_2$ (plus thermal conduction in the solid and the fluid). When there is a superimposed steady flow, there is an additional component of the enthalpy flux due to this steady flow, $\dot{H}_{\text{flow}} = \dot{m} h$, where $\dot{m}$ is the mass flow rate and h is the specific enthalpy of the fluid. Ignoring thermal conduction, conservation of energy has $\dot{Q}_2 + \dot{H}_{\text{flow}} = \text{const}$. If the acoustic fluid may be modeled as an ideal gas inside the stack, $h(T,p) = c_p T$, and the conservation-of-energy equation leads to an exponential mean temperature profile in the stack.[1]

More accurate calculations are done using the full one-dimensional linearized Navier–Stokes, continuity, and entropy equations using the numerical computation program DeltaE.[4] Extensions were made to the code to model fluids in multiple phases, in particular condensing humid air, and to compute enthalpy flows including the effect of steady flow.[5]

Above and below the stack, where there is no condensation, the humid air stream is modeled as a mixture of dry air and water vapor, taken as ideal gases. Complications arise inside the stack where the water is condensing, since the gas will be in close contact with liquid water, either as a film on the stack-channel walls, or as droplets in the gas. This can result in different (non-ideal-gas) values for thermodynamic derivatives such as the effective specific heat and thermal expansivity, which in turn can affect the rate of thermoacoustic heat pumping.

The exact computation of the various thermodynamic derivatives would in general require a knowledge of the distribution and dynamics of entrained water inside the stack. Here, to perform calculations in the acoustic approximation, two simplified models of possible behavior of the fluid inside the stack are used. In the ''fog'' model all the condensate is assumed to be in the form of droplets sufficiently small, and sufficiently finely and uniformly dispersed relative to the thermal penetration depth, as to be in instantaneous thermal equilibrium with the surrounding gas. In the ''wet-wall'' model all the condensate is assumed to be on the stack-channel walls, and the gas between these wet walls is assumed to have a saturation concentration of water vapor, at the local mean temperature.

II. FOG THERMOACOUSTICS

In the ''fog'' model the condensate is assumed to be in the form of tiny droplets, so that the foggy air can be treated as a single fluid. The droplets must be so small that they are perfectly entrained in the gas motion, and they must be so finely and uniformly dispersed in the gas that the properties of the gas do not vary appreciably in the spaces between neighboring droplets. In other words, the droplet-to-droplet spacing must be much smaller than the thermal diffusion length δ_k and the corresponding mass-diffusion length $\delta_D = \sqrt{2D_{12}/\omega}$, where D_{12} is the water–air binary diffusion coefficient. In this model, evaporation and condensation of these dispersed droplets contribute significantly to the effective thermal expansivity, specific heat, etc. of the composite fluid.

The instantaneous pressure, $p = p_m + \text{Re}\,[p_1 e^{i\omega t}]$, with p_1 complex to account for time phasing, is the sum of the partial pressures of air and water vapor. The water vapor is in equilibrium with the droplets, so its pressure is the saturation pressure at the instantaneous local temperature. (The liquid water droplets, however, are compressed above atmospheric pressure, having a pressure equal to the total local pressure, plus surface pressure $\Delta p = \alpha/2r$, where $\alpha = 0.0075$ J/m^2 is the surface tension for an air–water interface and r is the radius of the droplet. This elevated pressure does not significantly affect the thermodynamics or energy flows.)

Given p, T, and the mole fraction of water $\overline{x_w}$, other thermodynamic variables are computed:

the mole fraction of air:

$$\overline{x_a} = 1 - \overline{x_w}, \tag{4}$$

the mole fraction of water vapor:

$$\overline{x_g} = \overline{x_a} \frac{p_{\text{sat}}(T)}{p - p_{\text{sat}}(T)}, \tag{5}$$

the mole fraction of liquid water:

$$\overline{x_f} = \overline{x_w} - \overline{x_g}, \tag{6}$$

and the molar mass of the mixture:

$$M = \overline{x_a} M_a + (\overline{x_a} + \overline{x_f}) M_w . \tag{7}$$

Here $p_{\text{sat}}(T)$ is the saturation, or vapor, pressure of water at temperature T, and M_a and M_w are the molar masses of air and water.

The specific enthalpy h of the fluid is the sum of the enthalpies of the components,

$$h = \frac{\overline{x_a}\,\overline{h_a} + \overline{x_g}\,\overline{h_g} + \overline{x_f}\,\overline{h_f}}{M}, \tag{8}$$

where $\overline{h_a} = (291\ \text{J/mol}\cdot\text{K})T$ is the molar enthalpy of dry air near room temperature, $\overline{h_g}$ is taken as its saturation value, and $\overline{h_f}$ contains a first-order correction for compression,

$$\overline{h_f}(T,p) = \overline{h}_{f,\text{sat}}(T) + \overline{v_f}(p - p_{\text{sat}}(T)), \tag{9}$$

where $\overline{v_f}$ is the molar volume of liquid water. (This correction is small, $\lesssim 100$ ppm for temperatures and pressures in this apparatus.) The heat capacity is computed from this enthalpy as

$$c_p = \left(\frac{\partial h}{\partial T} \right)_{p, \overline{x_w}} . \tag{10}$$

The molar volume of the fluid is

$$\overline{v} = (\overline{x_a} + \overline{x_g}) \frac{\overline{R}\,\overline{T}}{p} + \overline{x_f}\,\overline{v_f}, \tag{11}$$

where $\overline{R}=8.314$ J/mol·K is the gas constant. The thermodynamic response functions (derivatives) may be calculated from the molar volume:

$$\kappa_T=\frac{-1}{\overline{v}}\left(\frac{\partial\overline{v}}{\partial p}\right)_{T,\overline{x}_w} \tag{12}$$

and

$$\beta=\frac{1}{\overline{v}}\left(\frac{\partial\overline{v}}{\partial T}\right)_{p,\overline{x}_w}. \tag{13}$$

The adiabatic index is computed as

$$\gamma=\left(1-\frac{T\beta^2\overline{v}}{M\kappa_T c_p}\right)^{-1}, \tag{14}$$

and the speed of sound is

$$a=\sqrt{\frac{\gamma\overline{v}}{M\kappa_T}}. \tag{15}$$

The thermal conductivity K of the fluid is taken as that of air, and is used to compute the thermal diffusivity,

$$\chi=K\overline{v}/Mc_p, \tag{16}$$

and the viscosity is taken as the viscosity of air, corrected for a suspension of water droplets with the Einstein equation,[6]

$$\eta=\eta_{\text{air}}(T)\left(1+\frac{5}{2}\frac{\overline{x}_f\overline{v}_f}{\overline{v}}\right). \tag{17}$$

No correction is made for the effect of water vapor on the viscosity, since this is much less than 1% at the temperatures in this apparatus.[7] Traditional studies of sound propagation in fog describe the extra attenuation[8] due to oscillating evaporation/condensation of the droplets, but here the ordinary viscous and thermal dissipation at the stack-channel walls is dominant.

For example, this model predicts that cooling humid air at 3 bar with a dew point of 300 K below its dew point results in an increase in c_p of 80%, an increase in $T\beta$ of 15%, and smaller changes in other properties. The large change in c_p occurs because a change in temperature (in the fog region) results in a large change in the fraction of water condensed, and thus a large change in enthalpy because of the latent heat of water. Such changes could have a dramatic effect on the stack's heat-pumping rate through δ_k, β, and ∇T_{crit} in Eq. (1).

The binary diffusion coefficient D_{12} for air and water is about 2.2×10^{-5} m^2/s at 1 atm and 300 K.[9,10] The coefficient varies inversely with the pressure,[10] so at the operating pressure of 3 bar, and at 300 K, the diffusion coefficient is approximately $D_{12}(3\text{ bar, }300\text{ K})=0.7\times10^{-5}$ m^2/s. The diffusive penetration depth at 40 Hz is $\delta_D=\sqrt{2D_{12}/\omega}=0.23$ mm, which is about the same as the viscous and thermal penetrations depths for this system $\delta_\nu=\sqrt{2\eta/\rho_m\omega}=0.21$ mm and $\delta_k=\sqrt{2K\rho_m c_p\omega}=0.24$ mm, compared with the stack plate half-spacing of 0.41 mm. The fog model would be applicable here only if the droplet density were at least ~10 droplets/$\delta_\kappa^3\sim10^{12}$ droplets/m^3. For $\overline{x}_f\sim0.01$, the droplet size would then be $\sim3\mu$m, comparable to typical sizes in atmospheric clouds.[11]

III. WET-WALL THERMOACOUSTICS

In the ''wet-wall'' model all of the condensate is assumed to be on the stack walls, and the gas between these wet walls is assumed to be saturated with water vapor at the local stack wall temperature.[9] As pressure and temperature oscillate in the gas, droplets do not form, even though the minima in the gas's temperature oscillations are slightly below the dew point. In this model (after a transient period during which water first builds up on the walls), the water that condenses in the stack must flow out of the cold end of the stack as liquid. We assume that this liquid flow is steady, driven by gravity and capillary forces, so that large droplets never occlude the stack channels.

In this model, we neglect any effects of *oscillating* diffusion of water vapor, even though the oscillating thermoacoustic temperature gradients must drive such diffusion, because the extra acoustic-power dissipation and time-averaged vapor pumping associated with the oscillating diffusion should be small at these small vapor mole fractions.[9,12] Nevertheless, we rely on *time-averaged* diffusion of water vapor from the center of the channels to the walls where it condenses. The gradient in water-vapor density that drives this diffusion can be estimated from the laminar steady-state velocity

$$u=\frac{3}{2}\frac{U}{A}\left(1-\frac{y^2}{y_0^2}\right) \tag{18}$$

between parallel plates of separation $2y_0$, with coordinate y measured from midway between the plates and A the cross-sectional area through which volume flow rate U passes. In this situation, the largest terms in the mass diffusion equation give

$$u\frac{d\overline{x}_g}{dz}=D_{12}\frac{d^2\overline{x}_g}{dy^2}, \tag{19}$$

where z is the direction of steady flow. The concentration gradient in the flow direction is related to the temperature gradient along the wet-wall channel by

$$\frac{d\overline{x}_g}{dz}\approx\frac{1}{p}\frac{dp_{\text{sat}}}{dT}\frac{dT}{dz}. \tag{20}$$

With boundary conditions $\overline{x}_g(\pm y_0)=\overline{x}_{g,\text{wall}}$, the solution to Eq. (19) using Eq. (18) for u is a quartic polynomial in y, which easily gives the water-vapor concentration difference between mid-channel and wall:

$$\overline{x}_g(0)-\overline{x}_{g,\text{wall}}=\frac{5}{8}\frac{y_0^2}{D_{12}}\frac{U}{A}\frac{1}{p}\frac{dp_{\text{sat}}}{dT}\frac{dT}{dz}. \tag{21}$$

For the conditions of the typical experiment described below, this concentration difference is only 10% of the concentration itself, and diffusion in the z direction carries 10^5 times less water than this diffusion in the y direction.

The effective thermal expansivity, specific heat, etc. used in calculations of thermoacoustic dynamics are simply those of an ideal gas mixture of air and water vapor, while only the enthalpy of the fluid used for computing the open-flow energy balance includes the effect of the condensate. The mole fractions of air and water vapor are computed from the mean temperature of the fluid:

$$\overline{x}_g = \frac{p_{\mathrm{sat}}(T_m)}{p_m} \tag{22}$$

and

$$\overline{x}_a = 1 - \overline{x}_g . \tag{23}$$

For calculations of oscillating variables these gases are assumed to act as an ideal gas, with a molar volume

$$\overline{v} = \frac{\overline{R}\overline{T}}{p}, \tag{24}$$

so

$$\beta = \frac{1}{\overline{T}} \tag{25}$$

and

$$\kappa_T = \frac{1}{p}. \tag{26}$$

The molar mass and heat capacity used for calculations of oscillating variables are weighted by the mole fractions:

$$M = \overline{x}_w M_w + \overline{x}_a M_a , \tag{27}$$

$$c_p = \frac{\overline{x}_a \overline{c}_{p,a} + \overline{x}_g \overline{c}_{p,g}}{M}, \tag{28}$$

where $\overline{c}_p$ is the heat capacity per mole at constant pressure. The adiabatic index and sound speed are computed from these variables as in the fog case.

While Eq. (28) is used for the calculation of oscillating quantities in the ''wet-wall'' model, the total enthalpy of the fluid is used for steady-flow energy balance to determine $T_m(z)$, and hence includes the effect of the condensate, most importantly the latent heat. Thus the steady-flow enthalpy is the same as in the fog case, above.

The thermal conductivity and viscosity are taken to be that of air at the same temperature and pressure.

A given parcel of gas is assumed to exist at constant mole fractions of air and water vapor at the fast (acoustic) time scale. The mole fractions vary slowly as this parcel of gas travels with the mean flow to regions of different mean temperature. This implies that during the rarefaction part of the cycle the water vapor becomes supersaturated, but does not condense. Practically, this means that the rate of nucleation of droplets is small.

IV. EXPERIMENT

A modification of the apparatus built by Reid is used to dehumidify air.[1] This thermoacoustic cooler is an annular resonator constructed of PVC piping with a circumference of 4.6 m along the wave-propagation direction, with an inner diameter ranging from 10 to 15 cm. A schematic drawing of the resonator is shown in Fig. 1. The working pressure of the air in the resonator is 3 atm.

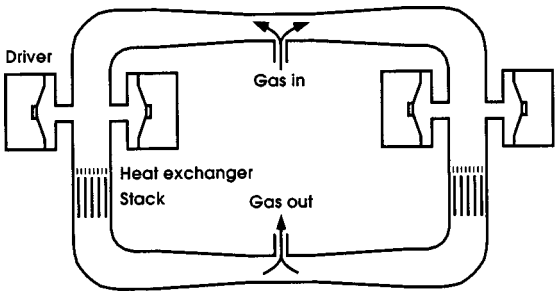

FIG. 1. Schematic diagram of the resonator. The sound field is left-right symmetric, with pressure nodes at the top and bottom centers, where the steady flow of gas may be introduced into or removed from the resonator. The duct is PVC piping, 150 mm ID, except near pressure nodes where it tapers to 100 mm ID. Acoustic energy is introduced with four 300-mm-diam woofers, driving the system near its resonance of 42 Hz. The stacks are parallel fiberglass sheets, 150 mm long, and spaced 0.81 mm apart. The ambient-temperature heat exchanger is water-cooled finned copper tubing.

Acoustic power is generated by four 300-mm-diam woofers operating near 42 Hz. The frequency is chosen to maximize the ratio of the stack temperature gradient at constant heat load to the acoustic work input to the resonator, which occurs close to the acoustic resonance frequency measured at very low power. The two woofers on each side are driven in phase, and the pairs of woofers on the two sides are driven out of phase to produce a standing wave with pressure nodes at the top and bottom, to allow the introduction and removal of the flowing gas without leakage of acoustic energy. At maximum drive without distortion the woofers produce a pressure amplitude $|p_1|/p_m = 0.025$, as measured by a pressure sensor placed between a pair of woofers. In this circumstance each woofer generates 12 W of acoustic power, with an electrical-to-acoustic efficiency of 20%. The overall second-law efficiency[13] of the heat pump is only about 1%—in other words, the electric power supplied to the woofers in order to cool the air is about 100 times larger than the minimum power required according to the first and second laws of thermodynamics.

Static and dynamic (acoustic) pressure are measured with piezoresistive pressure sensors placed in several locations around the resonator. By adjusting the voltage to the four woofers, the sound pressure amplitude may be made approximately equal in the two sides (to about 1%), and nulled at the pressure nodes at top and bottom (to about 0.01% of the maximum pressure amplitude in the resonator). The ''length'' of each half of the resonator from top pressure node to bottom pressure node is significantly less than $\frac{1}{2}$ wavelength, because the woofers are a substantial source of volume flow rate in quadrature with the oscillating pressure (roughly 30 times the in-phase volume flow rate that delivers acoustic power from the woofers to the resonator).

On each side of the resonator is a thermoacoustic stack, positioned about $\frac{1}{8}$ wavelength from the pressure node at the bottom. The stack is constructed of parallel plates of smooth fiberglass, with a length of 150 mm and a plate-to-plate separation of 0.81 mm maintained by axial spacers creating rectangular channels 0.81 mm by 12.7 mm in cross section. Just

above the stack is a copper fin-and-tube heat exchanger which is cooled to ambient temperature with a water stream. In the presence of the sound field, the stack produces a temperature gradient, with the colder end below.[3] Since the top of the stack is held at ambient temperature, the bottom of the stack is refrigerated. Humid air enters the resonator at the pressure node at the top, flows through the stack while transferring heat to the stack as it becomes colder, and exits the resonator at the pressure node at the bottom. Heat removed from the gas stream is pumped up the stack temperature gradient at the expense of acoustic energy, and is removed at the ambient-temperature heat exchanger.

The stack temperature profile is measured with ten thermocouple temperature sensors spaced along the (blocked) central channel of one stack. Additional temperature sensors are placed in the ambient heat exchanger metal, and in the gas space above and below the stack. Since the fluid is in close thermal contact with the stack, the local time-averaged temperature of the fluid inside the stack is assumed to be the same as that of the stack.

Humidity is measured with an Ohmic Instruments DPSC-35-XR Dew Point Meter, placed at the lower (outlet) port of the resonator. This detector uses a thin-film polymer capacitor exposed to the air stream, and reads relative humidity directly. The incoming humidity can be measured at the outlet with the acoustic drive off. In practice the hygrometer has limited utility because the PVC resonator material adsorbs or releases water, requiring many hours to equilibrate with the humid air stream.

All the runs are done with air, at varying humidity. House compressed air is used as the source of dry air, regulated down to the working pressure of the resonator and filtered through a plastic mesh having 8-μm square pores (not fine enough to remove typical condensation nuclei[11]). This source is well dehumidified, with a dew point at 3 bar of less than $-45\,^{\circ}\mathrm{C}$, the minimum detectable with the available hygrometer, for a specific humidity of less than 15 ppm. To obtain a desired humidity, this air stream is bubbled through liquid water of known, thermostat-controlled temperature. It is assumed that the exiting gas stream has a dew point equal to the temperature of the water, at a pressure equal to the pressure in the space above the liquid. The latent heat of the evaporated water is supplied by an electric heater.

Flow rates are measured using a laminar flow meter upstream of the humidifier. Since the incoming air stream is dry, this flow meter measures the (dry) air flow rate through the humidifier and resonator. The pressure drop across the element is proportional to the volume flow rate U and the viscosity of the gas, so

$$U = A\frac{\Delta p}{\eta/\eta_{70\,^{\circ}\mathrm{F}}}, \tag{29}$$

where A is a constant which depends on the geometry of the element, η is the dynamic viscosity, and $\eta_{70\,^{\circ}\mathrm{F}} = 182$ μ poise is the viscosity of air at $70\,^{\circ}\mathrm{F}$. The mass flow rate is computed from the density as an ideal gas,

$$\dot{m}_{\mathrm{air}} = U\rho_a = U\frac{p_{\mathrm{flow}}M_a}{\overline{R}T_{\mathrm{flow}}}, \tag{30}$$

where p_{flow} and T_{flow} are the pressure and temperature of the flowing air. After the humidifier, the mass flow rate of the fluid is

$$\dot{m} = \dot{m}_{\mathrm{air}} + \dot{m}_w = \dot{m}_{\mathrm{air}}(1+\Omega), \tag{31}$$

where $\Omega = \dot{m}_w/\dot{m}_{\mathrm{air}}$ is the specific humidity of the air downstream of the humidifier. This gas flow is assumed to split evenly through the two sides of the resonator, so the mass flow rate through each side is one-half of that calculated by Eq. (31).

When the flowing gas stream is humid air and the temperature anywhere inside the stack is below its dew point, liquid water will condense inside the stack. Since the flow is in close thermal contact with the stack plates, the gas stream will exit with a dew point equal to the temperature of the cold end of the stack. The condensate drains to the bottom of the stack. Water condensing in the stack is probably drawn into the corners of the stack's rectangular channels by capillary forces, so that most of the steady flow of liquid water down through the stack occurs in these corners. With a radius of curvature 0.4 mm typical of the channel corners, the surface tension of water reduces the pressure in the liquid by 200 Pa, in principle able to hold a 2-cm height of water against gravity.

In practice the cooler is started using flowing dry air, and it operates as an ordinary thermoacoustic flow-through cooler, with the air leaving the stack at the temperature of the cold end; the heat removed is pumped up the stack to be removed at the ambient-temperature heat exchanger. To operate the device as a dehumidifier the humidity of the incoming air may then be increased to reach an incoming dew point warmer than the coldest part of the stack. The temperature difference across the stack is observed to decrease because of the latent heat of the liquid condensing in the stack. Initially the dew point of the exiting air is measured to be the same as the cold-end stack temperature. Running this way for an hour will condense several grams of water in the stack. Eventually, the dew point of the exiting gas slowly rises, due to condensate appearing in the warmer sections of the resonator past the stack, signaling what we believe is the beginning of steady-state liquid holdup in the stack.

To determine the fate of this condensate, a 15-cm section of the resonator below the stack was replaced with transparent acrylic so the bottom (cold end) of the stack and the region below it could be seen. In addition, windows were installed in the resonator elbows above and below the stack to allow illumination or observation along the stack channels. The best view was obtained with a strong light above the stack (shining through the channels), observing through the acrylic resonator section.

Liquid water begins to appear as droplets on the bottom of the stack. The liquid water condensate at the bottom of the stack continues to accumulate, blocking some of the stack channels, and eventually falls away in a rain of millimeter-size or smaller drops. Cotton string, held against the bottom of the stack with a loose screen, was added to wick away the condensate, thereby eliminating the rain and preventing significant occlusion of the stack channels. The water drips off the ends of the dangling strings, and can be directed in this

way to a reservoir, from which it might be removed from the resonator. With this wick installed, viewing along the stack axis using the elbow windows shows no channels blocked by drops.

Under certain conditions, namely a very high incoming dew point (~35 °C, or around 10 °C higher than the temperature of the warmest part of the stack) and high air flow rate (~0.005 kg/s), a thin fog is seen exiting from the bottom of the stack. This fog can be seen best through the transparent duct below the stack, with strong illumination from above through the stack channels. The fog is visible in a region extending about 5 cm below the bottom of the stack, after which it presumably evaporates into the outgoing air stream. The fog appears about 30 min after introducing humidity into the operating resonator, and disappears after another 30 to 60 min, when significant amounts of liquid water (enough to occlude some stack pores) have appeared at the bottom of the stack. We suspect that this fog is created in the region roughly a peak-to-peak gas displacement amplitude (~2 cm) below the cold end of the stack, because the gas there is cooled some 6 °C below the temperature of the cold end of the stack by adiabatic pressure-displacement oscillations.

V. RESULTS AND DISCUSSION

To investigate the behavior of the air cooler/dehumidifier, the temperature profile along the stack is observed during operation. Of particular interest is the shape of the temperature profile in regions of the stack where water is, and is not, condensing. Figure 2 shows a temperature profile typical of those having the condensation line near the center of the stack, to show both dry and damp operation at the same time. Above this location the temperature of the stack is above the dew point of the incoming air so no condensation occurs. Below it condensation onto the stack keeps the local dew point equal to the local temperature of the stack.

Also shown are two calculations of the temperature profile using DeltaE.[4] These models use the actual geometry of the resonator around the stack, matching acoustic pressure amplitude and phase above and below the stack. The only free parameter is the additional parasitic heat load on the bottom of the stack due to convective streaming in the duct below. This parasitic heat load is fairly constant at about 20 W per side.

The two model curves represent DeltaE simulations using the ''fog'' and ''wet-wall'' computations for the enthalpy and thermodynamic derivatives of the air and liquid and gaseous water inside the stack. The kink in the fog-model curve is largely due to the large increase in c_p which occurs with the introduction of fog droplets. In the ''fog'' model, this abruptly lowers the critical temperature gradient according to the c_p dependence in Eq. (3), causing a corresponding abrupt change in dT_m/dz in Eq. (1) in order to keep the heat pumped continuous. In the ''wet-wall'' model, all variables in Eq. (1) are continuous at the dew point, so there is no discontinuity in dT_m/dz. The lack of this kink in the measured temperature profile suggests that the influence of droplets in this condensing thermoacoustic system is small

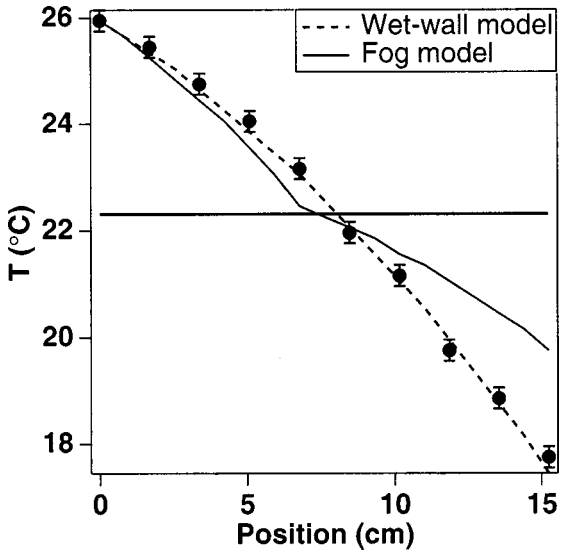

FIG. 2. Measured (markers) and simulated (lines) temperature distribution on one stack, with $|p_1|=7660$ Pa midway between the drivers above the stack and 0.001 kg/s of humid air flowing down through the stack, and with cotton string wick to prevent blockage of channels by drops. The curves are calculated using DeltaE: the solid curve represents the calculation assuming that the condensate is in the form of droplets (''fog''), and the dashed curve represents that with the condensate completely on the walls of the stack (''wet-wall''). The parasitic heat leak at the cold end (24 W) is the same for both curves, and is adjusted so the ''wet-wall'' curve matches the measured temperatures at the endpoints. For comparison, the calculation for dry air is hardly distinguishable from the ''wet-wall'' calculation, falling only 0.2 °C below it at the midpoint. The horizontal line is the dew point of the incoming air.

enough that the ''wet-wall'' model accurately describes this apparatus.

There are several reasons to expect that the ''wet-wall'' model is more applicable here than the ''fog'' model. In order to enforce the conditions of fog thermoacoustics, the distribution of water droplets must be sufficiently dense, so that most of the air in the thermoacoustically active region is close to a water droplet (much closer than a thermal or diffusive penetration depth). This would require that there be sufficient condensation nuclei to produce this density of droplets. Urban atmospheric air typically has 10^{11} nucleation-site impurities per cubic meter (mostly ionic ''Aitken nuclei,'' $r<200$ nm), and rural air is typically only an order of magnitude lower.[11] For the conditions of Fig. 2, 10^{11} droplets/m^3 results in only about 1 droplet/δ_k^3. This density would be too low to enforce ''fog'' behavior.

Moreover, any condensate that might form in droplets could tend to move to the stack walls, whether via streaming,[14] Stefan flow,[8,15] or diffusion. Continued condensation on droplets, and agglomeration due to collisions, would also tend to increase the size of the droplets, reducing their number so that the fog model would be invalid. (These effects might not, however, be important until several acoustic displacements below the condensation line, so that dense fog at the condensation line might still cause a kink in the temperature profile at the condensation line, even if the condensate were mostly on the walls below.)

If the observation of ''wet-wall'' thermoacoustics is indeed due to insufficient condensation nuclei, some predic-

tions may be made about the behavior of other condensing thermoacoustic systems. A small compressed air dryer, for example, would operate at the compressor pressure of 10–15 bar, and at a higher frequency than this device. Because of the higher pressure and frequency the penetration depths δ_k and δ_D would be smaller. If the same density of condensation nuclei were present, there would be even fewer droplets per δ_k^3, so ''wet-wall'' thermoacoustics would be even more strongly enforced. Other possible applications, such as lumber or grain drying, would probably use very large resonators operating at atmospheric pressure. In these systems low frequency and pressure lead to larger penetration depths, so that there could be enough condensation nuclei to produce many fog droplets per δ_k^3, and ''fog'' thermoacoustic behavior might occur.

The form of condensation in a particular thermoacoustic dehumidifier will have a strong influence on design. Condensate accumulating mostly on the stack plates is easier to remove, as in this experiment with wicks attached to the bottom of the stack. If the water were largely in the form of fog, some manner of capturing the small droplets would be required downstream of the stack to prevent the liquid entrained in the air stream from evaporating back into the dry air. In addition, the thermoacoustic heat pumping [Eq. (1)] and critical temperature gradient [Eq. (3)] may vary by 20% to 50% depending on the nature of the condensate, which may require substantial changes in stack length, spacing, and placement.

VI. CONCLUSION

We have demonstrated dehumidification of a humid air stream using a flow-through thermoacoustic cooler. While the efficiency is lower than commercial compressed air dehumidifiers using vapor-compression refrigeration, this approach promises the greater simplicity and reliability of thermoacoustic systems. The liquid condensate does not appear to affect the oscillating thermoacoustic variables, which can be described by ideal-gas equations, but the condensing water is a large thermal load on the refrigerator. The measured temperature profile is well fit by a model which assumes that all of the condensate is on the walls of the stack.

ACKNOWLEDGMENTS

We thank Bob Reid for the use of his thermoacoustic refrigerator, David Gardner for technical support, Rich Raspet for stimulating discussions, and Bill Ward for DeltaE support and modifications. This work was supported by the Office of Basic Energy Sciences in the U.S. Department of Energy.

[1] R. S. Reid, W. C. Ward, and G. W. Swift, ''Cyclic thermodynamics with open flow,'' Phys. Rev. Lett. **80**, 4617–4620 (1998); R. S. Reid and G. W. Swift, ''Experiments with a flow-through thermoacoustic refrigerator,'' submitted to J. Acoust. Soc. Am.

[2] O. T. Zimmerman and Irvin Lavine, *Psychrometric Tables and Charts* (Industrial Research Service, Dover, 1964).

[3] G. W. Swift, ''Thermoacoustic engines,'' J. Acoust. Soc. Am. **84**, 1145–1180 (1988).

[4] W. C. Ward and G. S. Swift, ''Design environment for low-amplitude thermoacoustic engines,'' J. Acoust. Soc. Am. **95**, 3671–3672 (1994). To review DeltaE's capabilities, visit http://www.lanl.gov/thermoacoustics/. For a beta-test version, contact ww@lanl.gov (Bill Ward) or swift@lanl.gov (Greg Swift). Fully tested software available from ESTSC, US DOE, Oak Ridge, TN.

[5] W. C. Ward (unpublished).

[6] L. D. Landau and E. M. Lifshitz, *Fluid Mechanics* (Pergamon, Oxford, 1987).

[7] J. Kestin and J. H. Whitelaw, ''The viscosity of dry and humid air,'' Int. J. Heat Mass Transf. **7**, 1245–1255 (1964).

[8] N. A. Fuchs, *The Mechanics of Aerosols* (Pergamon, Oxford, 1964).

[9] R. Raspet, C. J. Hickey, and J. M. Sabatier, ''The effect of evaporation-condensation on sound propagation in cylindrical tubes using the low reduced frequency approximation,'' J. Acoust. Soc. Am. **105**, 65–73 (1999).

[10] J. O. Hirschfelder, C. F. Curtiss, and R. B. Bird, *Molecular Theory of Gases and Liquids* (Wiley, New York, 1954).

[11] B. J. Mason, *The Physics of Clouds* (Oxford U. P., Oxford, 1957).

[12] G. W. Swift and P. S. Spoor, ''Thermal diffusion and mixture separation in the acoustic boundary layer,'' J. Acoust. Soc. Am. **106**, 1794–1800 (1999).

[13] A. Bejan, *Advanced Engineering Thermodynamics*, 2nd ed. (Wiley, New York, 1997).

[14] W. L. M. Nyborg, ''Acoustic Streaming,'' in *Physical Acoustics*, edited by W. P. Mason (Academic, New York, 1965), Vol. IIB, pp. 265–331.

[15] D. Camuffo, *Microclimate for Cultural Heritage* (Elsevier, Amsterdam, 1998).